SAND--97-8542C

ANALYSIS OF HYDRODYNAMIC (LANDAU) INSTABILITY IN LIQUID-PROPELLANT COMBUSTION AT NORMAL AND REDUCED GRAVITY

CONF-9705199--

RECEIVED
SEP 29 1997
OSTI

STEPHEN B. MARGOLIS
Combustion Research Facility, MS 9052
Sandia National Laboratories, Livermore, California 94551-0969

Introduction

The burning of liquid propellants is a fundamental combustion problem that is applicable to various types of propulsion and energetic systems. The deflagration process is often rather complex, with vaporization and pyrolysis occurring at the liquid/gas interface and distributed combustion occurring either in the gas phase[1] or in a spray.[2] Nonetheless, there are realistic limiting cases in which combustion may be approximated by an overall reaction at the liquid/gas interface. In one such limit, the gas flame occurs under near-breakaway conditions, exerting little thermal or hydrodynamic influence on the burning propellant. In another such limit, distributed combustion occurs in an intrusive regime, the reaction zone lying closer to the liquid/gas interface than the length scale of any disturbance of interest. Finally, the liquid propellant may simply undergo exothermic decomposition at the surface without any significant distributed combustion, such as appears to occur in some types of hydroxylammonium nitrate (HAN)-based liquid propellants at low pressures.[3] Such limiting models have recently been formulated,[4,5] thereby significantly generalizing earlier classical models[6,7] that were originally introduced to study the hydrodynamic stability of a reactive liquid/gas interface. In all of these investigations, gravity appears explicitly and plays a significant role, along with surface tension, viscosity, and, in the more recent models, certain reaction-rate parameters associated with the pressure and temperature sensitivities of the reaction itself. In particular, these parameters determine the stability of the deflagration with respect to not only classical hydrodynamic disturbances, but also with respect to reactive/diffusive influences as well. Indeed, the inverse Froude number, representing the ratio of buoyant to inertial forces, appears explicitly in all of these models, and consequently, in the dispersion relation that determines the neutral stability boundaries beyond which steady, planar burning is unstable to nonsteady, and/or nonplanar (cellular) modes of burning.[8,9]. These instabilities thus lead to a number of interesting phenomena, such as the sloshing type of waves that have been observed in mixtures of HAN and triethanolammonium nitrate (TEAN) with water.[3] Although the Froude number was treated as an O(1) quantity in these studies, the limit of small inverse Froude number corresponding to the microgravity regime is increasingly of interest and can be treated explicitly, leading to various limiting forms of the models, the neutral stability boundaries, and, ultimately, the evolution equations that govern the nonlinear dynamics of the propagating reaction front. In the present work, we formally exploit this limiting parameter regime to compare some of the features of hydrodynamic instability of liquid-propellant combustion at reduced gravity with the same phenomenon at normal gravity.

Mathematical Formulation

The starting point for the present work is our recent model[4,5] that generalizes classical models[6,7] of a reactive liquid/gas interface by replacing the simple assumption of a fixed normal propagation speed with a reaction/pyrolysis rate that is a function of the local pressure and temperature. This introduces important new sensitivity parameters that couple the local burning rate with the pressure and temperature fields. Thus, it is assumed, as in the classical models, that there is no distributed reaction in either the liquid or gas phases, but that there exists either a pyrolysis reaction or an exothermic decomposition at the liquid/gas interface that depends on local conditions there. In its most general form, the model includes full heat and momentum transport, allowing for viscous effects in both the liquid and gas phases, as well as effects due to gravity and surface tension. For additional simplicity, however, it is assumed that within the liquid and gas phases separately, the density, heat capacity, kinematic viscosity and thermal diffusivity are constants, with appropriate jumps in these quantities across the phase boundary.

The nondimensional location of this interface as a function of space and time is denoted by $x_3 = \Phi_s(x_1, x_2, t)$, where the adopted coordinate system is fixed with respect to the stationary liquid at $x_3 = -\infty$ (Figure 1). Then, in the moving coordinate system $x = x_1$, $y = x_2$, $z = x_3 - \Phi_s(x_1, x_2, t)$, in terms of which the liquid/gas interface always lies at $z = 0$, the complete formulation of the problem is given as follows. Conservation of mass, energy and momentum within each phase imply

$$\nabla \cdot \mathbf{v} = 0, \quad z \neq 0, \qquad \frac{\partial \Theta}{\partial t} - \frac{\partial \Phi_s}{\partial t}\frac{\partial \Theta}{\partial z} + \mathbf{v} \cdot \nabla \Theta = \begin{Bmatrix} 1 \\ \lambda \end{Bmatrix} \nabla^2 \Theta, \quad z \lessgtr 0, \tag{1,2}$$

DISTRIBUTION OF THIS DOCUMENT IS UNLIMITED

MASTER

DISCLAIMER

This report was prepared as an account of work sponsored by an agency of the United States Government. Neither the United States Government nor any agency thereof, nor any of their employees, makes any warranty, express or implied, or assumes any legal liability or responsibility for the accuracy, completeness, or usefulness of any information, apparatus, product, or process disclosed, or represents that its use would not infringe privately owned rights. Reference herein to any specific commercial product, process, or service by trade name, trademark, manufacturer, or otherwise does not necessarily constitute or imply its endorsement, recommendation, or favoring by the United States Government or any agency thereof. The views and opinions of authors expressed herein do not necessarily state or reflect those of the United States Government or any agency thereof.

DISCLAIMER

Portions of this document may be illegible in electronic image products. Images are produced from the best available original document.

$$\frac{\partial \mathbf{v}}{\partial t} - \frac{\partial \Phi_s}{\partial t}\frac{\partial \mathbf{v}}{\partial z} + (\mathbf{v}\cdot\nabla)\mathbf{v} = (0,0,-Fr^{-1}) - \left\{ \begin{matrix} 1 \\ \rho^{-1} \end{matrix} \right\} \nabla p + \left\{ \begin{matrix} Pr_l \\ \lambda Pr_g \end{matrix} \right\} \nabla^2 \mathbf{v}, \quad z \lesseqgtr 0, \tag{3}$$

where $\mathbf{v}$, Θ and p denote velocity, temperature and pressure, respectively, $Pr_{l,g}$ denote the liquid and gas-phase Prandtl numbers, ρ, λ and c (used below) are the gas-to-liquid density, thermal diffusivity and heat-capacity ratios, and Fr is the Froude number.

The above equations are subject to the boundary conditions $\mathbf{v} = \mathbf{0}$, $\Theta = 0$ at $z = -\infty$, $\Theta = 1$ at $z = +\infty$, $\Theta|_{z=0-} = \Theta|_{z=0+}$, and appropriate jump and continuity conditions at the liquid/gas interface. The latter consist of continuity of the transverse velocity components (no-slip) and conservation of (normal) mass flux,

$$\hat{\mathbf{n}}_s \times \mathbf{v}_- = \hat{\mathbf{n}}_s \times \mathbf{v}_+, \quad \hat{\mathbf{n}}_s\cdot(\mathbf{v}_- - \rho\mathbf{v}_+) = (1-\rho)S(\Phi_s)\frac{\partial \Phi_s}{\partial t}, \tag{4,5}$$

the mass burning rate (pyrolysis) law,

$$\hat{\mathbf{n}}_s\cdot\mathbf{v}_- - S(\Phi_s)\frac{\partial \Phi_s}{\partial t} = A(\Theta|_{z=0}, p|_{z=0+})\exp\left[\frac{N(1-\sigma_u)(\Theta|_{z=0}-1)}{\sigma_u + (1-\sigma_u)\Theta|_{z=0}}\right], \tag{6}$$

and conservation of the normal and transverse components of momentum and heat fluxes,

$$\begin{aligned} p|_{z=0-} - p|_{z=0+} = {} & \hat{\mathbf{n}}_s\cdot[\rho\mathbf{v}_+(\hat{\mathbf{n}}_s\cdot\mathbf{v}_+) - \mathbf{v}_-(\hat{\mathbf{n}}_s\cdot\mathbf{v}_-) - \rho\lambda Pr_g \mathbf{e}_+\cdot\hat{\mathbf{n}}_s + Pr_l \mathbf{e}_-\cdot\hat{\mathbf{n}}_s] + \hat{\mathbf{n}}_s\cdot(\mathbf{v}_- - \rho\mathbf{v}_+)S(\Phi_s)\frac{\partial \Phi_s}{\partial t} \\ & - \gamma S^3(\Phi_s)\left\{\frac{\partial^2\Phi_s}{\partial x^2}\left[1+\left(\frac{\partial\Phi_s}{\partial y}\right)^2\right] + \frac{\partial^2\Phi_s}{\partial y^2}\left[1+\left(\frac{\partial\Phi_s}{\partial x}\right)^2\right] - 2\frac{\partial\Phi_s}{\partial x}\frac{\partial\Phi_s}{\partial y}\frac{\partial^2\Phi_s}{\partial x\partial y}\right\}, \end{aligned} \tag{7}$$

$$\hat{\mathbf{n}}_s\times\left[\rho\mathbf{v}_+(\hat{\mathbf{n}}_s\cdot\mathbf{v}_+) - \mathbf{v}_-(\hat{\mathbf{n}}_s\cdot\mathbf{v}_-) + (\mathbf{v}_- - \rho\mathbf{v}_+)S(\Phi_s)\frac{\partial\Phi_s}{\partial t}\right] = \hat{\mathbf{n}}_s\times(\rho\lambda Pr_g\mathbf{e}_+\cdot\hat{\mathbf{n}}_s - Pr_l\mathbf{e}_-\cdot\hat{\mathbf{n}}_s), \tag{8}$$

$$\hat{\mathbf{n}}_s\cdot(c\rho\lambda\nabla\Theta|_{z=0+} - \nabla\Theta|_{z=0-}) = \hat{\mathbf{n}}_s\cdot\left[(c\rho\mathbf{v}_+ - \mathbf{v}_-)\Theta|_{z=0} + \hat{c}(\sigma_u\rho\mathbf{v}_+ - \mathbf{v}_-)\right] + \left[(1-c\rho)\Theta|_{z=0} + \hat{c}(1-\sigma_u\rho)\right]S(\Phi_s)\frac{\partial\Phi_s}{\partial t}, \tag{9}$$

where $\hat{c} = c/(1-\sigma_u)$, $\mathbf{e}$ is the rate-of-strain tensor, γ is the surface tension, σ_u is the unburned-to-burned temperature ratio, N is the nondimensional activation energy, A is the temperature- and pressure-dependent reaction-rate coefficient, $S(\Phi_s) \equiv [1 + (\partial\Phi_s/\partial x)^2 + (\partial\Phi_s/\partial y)^2]^{-1/2}$, and the unit normal $\hat{\mathbf{n}}_s = (-\partial\Phi_s/\partial x, -\partial\Phi_s/\partial y, 1)S(\Phi_s)$. Here, the gradient operator ∇ and the Laplacian ∇^2 are given in the moving coordinate system by

$$\nabla = \left(\frac{\partial}{\partial x} - \frac{\partial\Phi_s}{\partial x}\frac{\partial}{\partial z}, \frac{\partial}{\partial y} - \frac{\partial\Phi_s}{\partial y}\frac{\partial}{\partial z}, \frac{\partial}{\partial z}\right),$$

$$\nabla^2 = \frac{\partial^2}{\partial x^2} + \frac{\partial^2}{\partial y^2} + \frac{1}{S^2}\frac{\partial^2}{\partial z^2} - 2\frac{\partial\Phi_s}{\partial x}\frac{\partial^2}{\partial x\partial z} - 2\frac{\partial\Phi_s}{\partial y}\frac{\partial^2}{\partial y\partial z} - \left(\frac{\partial^2\Phi_s}{\partial x^2} + \frac{\partial^2\Phi_s}{\partial y^2}\right)\frac{\partial}{\partial z}.$$

However, the vector $\mathbf{v}$ still denotes the velocity with respect to the (x_1, x_2, x_3) coordinate system.

The Basic Solution and Classical Stability Results

A nontrivial basic solution to the above problem, corresponding to the special case of a steady, planar deflagration, is given by $\Phi_s^0 = -t$ and

$$\mathbf{v}^0 = (0,0,v^0), \quad v^0 = \begin{cases} 0, & z<0 \\ \rho^{-1}-1, & z>0, \end{cases} \quad \Theta^0(z) = \begin{cases} e^z, & z<0 \\ 1 & z>0, \end{cases} \quad p^0(z) = \begin{cases} -Fr^{-1}z + \rho^{-1} - 1, & z<0 \\ -\rho Fr^{-1}z, & z>0. \end{cases} \tag{10}$$

The linear stability analysis of this solution now proceeds in a standard fashion. However, owing to the significant number of parameters, a complete analysis of the resulting dispersion relation is quite complex. Realistic limits that may be exploited to facilitate the analysis include $\rho \ll 1$, $Pr_g/Pr_l \ll 1$, and in the microgravity regime, $Fr^{-1} \ll 1$.

In the study due to Landau,[6] the effects of gravity (assumed to act normal to the undisturbed planar interface in the direction of the unburned liquid) and surface tension were shown to be stabilizing, leading to a criterion for the absolute stability for steady, planar deflagration of the form (in our nondimensional notation) $4\gamma Fr^{-1}\rho^2/(1-\rho) > 1$. In the study due to Levich,[7] surface tension was neglected, but the effects due to the viscosity of the liquid were included, leading to the absolute stability criterion $Fr^{-1}Pr_l(3\rho)^{3/2} > 1$. Thus, these two studies, under the assumption of a constant

normal burning rate, demonstrated that sufficiently large values of either viscosity or surface tension, when coupled with the effects due to gravity, may render steady, planar deflagration stable to hydrodynamic disturbances. In the present work, we shall focus, using our extended model described above, primarily on hydrodynamic (Landau) instability. Thus, in the linear stability analysis, we retain only the pressure sensitivity $A_p \equiv \partial A/\partial p|_{\Theta=1,p=0}$ in the pyrolysis law (4), neglecting the temperature sensitivity $\Xi = N(1-\sigma_u) + A_\Theta$, where $A_\Theta \equiv \partial A/\partial\Theta|_{\Theta=1,p=0}$. The latter assumption thus filters out reactive/diffusive instabilities associated with the thermal coupling of the temperature field,[4,5] but facilitates the analysis of instability due to hydrodynamic effects alone. We note that the mass burning rate of many propellants has been shown empirically to correlate well with pressure.

Formal Analysis of the Zero-Viscosity Limit

In the limit of zero viscosities ($Pr_l = Pr_g = 0$), our extended model differs from the classical one due to Landau[6] only in the local pressure sensitivity of the normal burning rate. In that limit, the neutral stability boundaries with respect to infinitesimal hydrodynamic disturbances proportional to $e^{i\omega t \pm i\mathbf{k}\cdot\mathbf{x}}$, where $\mathbf{k}$ and $\mathbf{x}$ are the transverse wavenumber and coordinate vectors, respectively, are exhibited in Figure 2. Steady, planar burning is always unstable for positive values of A_p, but in the region $A_p \leq 0$, there exist both cellular ($\omega = 0$) and pulsating ($\omega \neq 0$) stability boundaries $A_p(k;\rho,\gamma,Fr^{-1})$ given by[5]

$$A_p = \rho\frac{\rho(1-\rho)Fr^{-1} + \rho\gamma k^2 - (1-\rho)k}{\rho^2(3-\rho)Fr^{-1} + \rho^2\gamma k^2 + (1-\rho)(2-\rho)k} \leq 0 \tag{11}$$

and $A_p = -\rho/(1-\rho)$, respectively, where $k = |\mathbf{k}|$. Steady, planar combustion is thus stable in the region $A_p < 0$ that lies between these two curves. The pulsating stability boundary is a straight line in the (A_p, k) plane, whereas the cellular stability boundary is a curve which lies at or above the straight line $A_p = -\rho/(2-\rho)$. The shape of the latter boundary depends on whether or not the parameters Fr^{-1} and/or γ are zero. In the limit that γFr^{-1} approaches the value $(1-\rho)/4\rho^2$ from below, the cellular stability boundary recedes from the region $A_p < 0$. For $\gamma Fr^{-1} > (1-\rho)/4\rho^2$, the stable region is the strip $-\rho/(1-\rho) < A_p < 0$. Thus, when $A_p = 0$, the classical Landau result for cellular instability is recovered. However, even a small positive value of A_p renders steady, planar burning intrinsically unstable for all disturbance wavenumbers, regardless of the stabilizing effects of gravity and surface tension. This result may be anticipated from quasi-steady physical considerations. That is, a burning velocity that increases with increasing pressure is a hydrodynamically unstable situation, since an increase in the burning velocity results in an increase in the pressure jump across the liquid/gas interface, and vice-versa. However, a sufficiently large negative value of A_p results in a pulsating hydrodynamic instability, the existence of which was a new prediction for liquid-propellant combustion. Zero and negative values of A_p over certain pressure ranges are characteristic of the so-called "plateau" and "mesa" types of solid propellants,[10] as well as for the HAN-based liquid propellants mentioned above.[3]

Of particular interest in the present work is the hydrodynamic stability of liquid-propellant combustion in the limit of small gravitational effects (*i.e.*, microgravity). In this limit, the shape of the upper hydrodynamic stability boundary in Figure 2, corresponding to the classical Landau instability, clearly approximates the $Fr^{-1} = 0$ curve except for small wavenumbers, where, unless the inverse Froude number is identically zero, the neutral stability boundary must turn and intersect the horizontal axis. Consequently, the neutral stability boundary has a minimum for some small value of the transverse wavenumber k of the disturbance, implying loss of stability of the basic solution to long wavelength perturbations as the pressure sensitivity A_p defined above decreases in magnitude. This, in turn, suggests a small wavenumber nonlinear stability analysis in the unstable regime, which generally leads to simplified nonlinear evolution equations of the Kuramoto-Sivashinsky type for the finite amplitude perturbations.[13,14]

To establish the nature of hydrodynamic instability in the microgravity regime in a formal sense, we may realistically consider the parameter regime $\rho \ll 1$, $Fr^{-1} \ll 1$, with $Fr^{-1} \sim \rho$. For example, typical values are $\rho \sim 10^{-3} - 10^{-4}$, liquid thermal diffusivity $\tilde{\lambda}_l \sim 0.1$ m^2/sec, and the steady, planar burning rate $\tilde{U} \sim 1 - 10$ cm/sec depending on pressure.[3] Hence, from the definition $Fr^{-1} \equiv \tilde{g}\tilde{\lambda}_l/\tilde{U}^3$, we conclude that $Fr^{-1} \sim \rho$ implies that the dimensional gravitational acceleration $\tilde{g} \lesssim 10^{-5}$ m/sec^2, which marks the onset of the microgravity regime. Thus, introducing the bookkeeping parameter $\epsilon \ll 1$, we define scaled parameters g^*, ρ^* and A_p^* according to $\rho = \rho^*\epsilon$, $Fr^{-1} = g^*\epsilon$ and $A_p = A_p^*\epsilon$. In that regime, it is readily seen from Eq. (11) that there are three distinct wavenumber scales: an inner scale $k_i = k/\epsilon^2$, the outer scale k, and a far outer scale $k_f = k\epsilon$. In the thin inner and thick far outer regions, we thus obtain

$$A_p^* \sim A_p^{*(i)} \sim \frac{\rho^*(\rho^* g^* - k_i)}{2k_i} \quad \text{and} \quad A_p^* \sim A_p^{*(f)} \sim \frac{1}{2}\rho^*(\rho^*\gamma k_f - 1)\,, \tag{12}$$

respectively. Each of these expansions may be matched to the O(1) outer expansion $A_p^* \sim A_p^{*(o)} \sim -\rho^*/2$, and thus a

composite expansion $A_p^{*(c)}(k)$ may be constructed as

$$A_p^{*(c)} \sim A_p^{*(i)} + A_p^{*(o)} + A_p^{*(f)} - \lim_{k_i \to \infty} A_p^{*(i)} - \lim_{k_f \to 0} A_p^{*(f)} \sim -\frac{1}{2}\rho^* + \frac{1}{2}\epsilon\rho^{*2}\gamma k + \epsilon^2 \frac{\rho^{*2} g^*}{2k}, \tag{13}$$

where the definitions of k_i and k_f have been used to express the final result in terms of k (Figure 3). Thus, the hydrodynamic stability boundary in the microgravity regime considered here lies in the region $A_p^* \leq 0$, intersecting the $A_p^* = 0$ axis at $k \sim 1/(\rho^*\gamma\epsilon) \gg 1$ and at $k \sim \rho^* g^* \epsilon^2 \ll 1$, with a single local minimum at $k \sim \sqrt{\epsilon g^*/\gamma} \sim 1/\sqrt{\gamma Fr} \sim O(\sqrt{\epsilon})$. Thus, instability first occurs for long wave disturbances at the critical value $A_p^* \sim -\rho^*/2 + \rho^{*2}\sqrt{g^*\gamma}\,\epsilon^{3/2}$ (*i.e.*, at $A_p \sim -\rho/2 + \rho^2\sqrt{\gamma/Fr}$).

Hydrodynamic Stability of the Full Model

Guided by these results for the inviscid case, the linear stability analysis may be extended to include the effects of viscosity as follows. Retaining the above scalings, we note that $\rho\lambda Pr_g = \mu Pr_l$, where $\mu = \mu_g/\mu_l$ is the gas-to-liquid viscosity ratio. Thus, it is reasonable to treat $Pr_l \equiv P$ as an O(1) parameter, and to consider the limit $\mu = \mu^*\epsilon \ll 1$. Introducing these scalings directly into the linear stability problem obtained from the linearization of the model about the basic solution (8), solutions may be sought in the form of appropriate expansions in powers of ϵ.[15] Proceeding in this fashion, we find that the hydrodynamic stability boundary in the small and intermediate wavenumber regimes is, to leading order, identical to that given above for the inviscid case, while this boundary in the large wavenumber regime, reflecting the influence of viscous effects, is given by

$$A_p^{*(f)} \sim -\rho^* + \frac{2\rho^*\mu^* P\left[1 + k_f(\rho^*\gamma + 2\mu^* P + 2\rho^* P)\right]}{4\mu^* P(1 + \rho^* P k_f) - (1 - R)(\rho^*\gamma + 2\mu^* P)}, \quad R = \left[1 + 4\mu^{*2} P^2 k_f^2\right]^{1/2}. \tag{14}$$

A composite expansion is thus constructed as in Eq. (13), giving the result

$$A_p^{*(c)} \sim \epsilon^2 \frac{\rho^{*2} g^*}{2k} - \rho^* + \frac{2\rho^*\mu^* P\left[1 + \epsilon k(\rho^*\gamma + 2\mu^* P + 2\rho^* P)\right]}{4\mu^* P(1 + \epsilon k\rho^* P) - (\rho^*\gamma + 2\mu^* P)\left[1 - (1 + 4\mu^{*2} P^2 \epsilon^2 k^2)^{1/2}\right]}. \tag{15}$$

The corresponding result for normal gravity is obtained by replacing the scaled gravity ϵg^* with the O(1) parameter Fr^{-1}, and both the normal and reduced gravity boundaries are graphically exhibited in Figure 4 for various zero and representative nonzero values of μ^*, P, Fr^{-1} and γ. It is readily seen that the essential qualitative difference between the normal and reduced-gravity curves is the location of the critical wavenumber for instability. Specifically, it is readily shown from Eq. (15) that the minimum in the neutral stability boundaries occurs for O(1) values of k under normal gravity, and at $k \sim O(\epsilon^{1/2})$ in the reduced-gravity limit, as in the inviscid case described above. Indeed, it may be shown that Eq. (15) collapses to Eq. (13) in the limit of zero viscosity ($P \to 0$), but it is now seen that viscous effects in *both* the liquid (P) and gas ($\mu^* P$) are comparable to surface-tension effects (γ) in damping large wavenumber disturbances. The equal importance of gas-phase viscosity relative to that of the liquid phase may be shown to arise from the fact that gas-phase disturbances are larger in magnitude than those in the liquid, such that a weak damping of a larger magnitude disturbance is of equal importance as an O(1) damping of a smaller magnitude disturbance.[15] The result (15) thus synthesizes and significantly extends the classical Landau/Levich results,[6,7] not only in allowing for a dynamic dependence of the burning rate on local conditions in the vicinity of the liquid/gas interface, but also in its formal treatment of those processes (surface tension, liquid and gas-phase viscosity) that affect damping of large-wavenumber disturbances.

Other cellular and pulsating stability boundaries are obtained[5] for nonzero values of the temperature sensitivity parameter Ξ, and are thus of a reactive/diffusive nature since they arise from a coupling of the burning rate to the local temperature field. These have been analyzed in the realistic limit $\rho \ll 1$ for the inviscid case,[5] and the generalization of these results to the fully viscous problem in both the normal and reduced-gravity regimes is currently under investigation. One important result obtained from the inviscid analysis is that the effect of nonzero thermal sensitivity Ξ turns out to have little bearing on the hydrodynamic cellular stability boundaries shown in Figures 2 – 4, while O(1) values of this parameter remove the hydrodynamic pulsating boundary to large negative values of A_p. Thus, it is the upper stability boundary in Figure 2, corresponding to the onset of steady cells on the propellant surface, that is the hydrodynamic instability of interest. An analysis of nonlinear stability in the neighborhood of this boundary[8,9] not only confirms the existence of steady cellular structures above this boundary, but also demonstrates how the interaction of certain types

of cellular modes can result in secondary and tertiary transitions to time-periodic motions[11–13] that may correspond to the sloshing type of behavior observed in HAN/TEAN/water mixtures.[3]

Conclusion

The present work has described a formal treatment of hydrodynamic instability in liquid-propellant combustion in both the normal and reduced-gravity parameter regimes. Exploiting the smallness of the gas-to-liquid density ratio, an asymptotic treatment of a generalized Landau/Levich - type model that allowed for a dynamic dependence of the burning rate on local perturbations was described. It was shown that there were three distinct wavenumber regimes to be considered, with different physical process assuming dominance in each. In particular, it was shown that the gravitational acceleration (assumed to be normal to the undisturbed liquid/gas interface in the direction of the liquid) is responsible for stabilizing long-wave disturbances, whereas surface tension and viscosity are effective in stabilizing short-wave perturbations. As a consequence, reduced gravity results in a shift in the minimum of the neutral stability boundary towards smaller wavenumbers, such that the onset of hydrodynamic instability, predicted to occur for sufficiently small negative values of the pressure-sensitivity coefficient A_p, becomes a long-wave instability in that limit. An additional result is that gas-phase viscosity plays an equally large role as liquid viscosity in the large wavenumber regime. This important effect, absent from previous treatments, stems from the fact that gas-phase disturbances are larger in magnitude than those in the liquid phase. Consequently, although the gas-to-liquid viscosity ratio is small, a weak damping of a larger magnitude disturbance is of equal importance to an O(1) damping of a smaller magnitude disturbance. In addition, the inclusion of both viscous and surface-tension effects in a single analysis, which are of comparable importance for short-wave perturbations, represents an important synthesis of the classical Landau/Levich theories.

Acknowledgment

This work was supported by the NASA Microgravity Science Research Program under contract C-32031-E.

References

1. Ya. B. Zel'dovich, G. I. Barenblatt, V. B. Librovich and G. M. Makhviladze, *The Mathematical Theory of Combustion and Explosions*, Consultants Bureau, New York, 1985.
2. F. A. Williams, *Combustion Theory*, Benjamin/Cummings, Menlo Park, 1985.
3. S. R. Vosen, *The Burning Rate of Hydroxylammonium Nitrate Based Liquid Propellants*, Twenty-Second Symposium (International) on Combustion (1989), 1817–1825.
4. R. C. Armstrong and S. B. Margolis, *Hydrodynamic and Reactive/Diffusive Instabilities in a Dynamic Model of Liquid Propellant Combustion*, Twenty-Second Symposium (International) on Combustion (1989), 1807–1815.
5. R. C. Armstrong and S. B. Margolis, *Hydrodynamic and Reactive/Diffusive Instabilities in a Dynamic Model of Liquid Propellant Combustion—II. Inviscid Fluid Motions*, Combust. Flame **77** (1989), 123-138.
6. L. D. Landau, *On the Theory of Slow Combustion*, Acta Physicochimica URSS **19** (1944), 77-85; Zh. Eksp. i Teor. Fiz. **14**, 240.
7. V. G. Levich, *On the Stability of the Flame Front When a Liquid is Burning Slowly*, Dokl. Akad. Nauk SSSR **109** (1956), pp. 975–978.
8. S. B. Margolis, G. I. Sivashinsky, and J. K. Bechtold, *Secondary Infinite-Period Bifurcation of Spinning Combustion Waves Near a Hydrodynamic Cellular Stability Boundary*, Physica D **43** (1990), 181–198.
9. J. K. Bechtold and S. B. Margolis, *Nonlinear Hydrodynamic Stability and Spinning Deflagration of Liquid Propellants*, SIAM J. Appl. Math. **51** (1991), 1356–1379.
10. Y. M. Timnat, *Advanced Chemical Rocket Propulsion*, Academic Press, London, 1987.
11. T. Erneux and E. L. Reiss, *Splitting of Steady Multiple Eigenvalues may Lead to Periodic Cascading Bifurcation*, SIAM J. Appl. Math. **43** (1983), 613–624.
12. J. D. Buckmaster, *Polyhedral Flames—an Exercise in Bimodal Bifurcation Analysis*, SIAM J. Appl. Math. **44** (1984), 40–55.
13. S. B. Margolis and G. I. Sivashinsky, *On Spinning Propagation of Cellular Flames*, Combust. Sci. Tech. **69** (1990), 99–131.
14. S. B. Margolis and G. I. Sivashinsky, *Flame Propagation in Vertical Channels: Bifurcation to Bimodal Cellular Flames*, SIAM J. Appl. Math. **44** (1984), 344–368.
15. S. B. Margolis, *Hydrodynamic Instability in an Extended Landau/Levich Model of Liquid-Propellant Combustion at Normal and Reduced Gravity*, submitted for publication (1997).

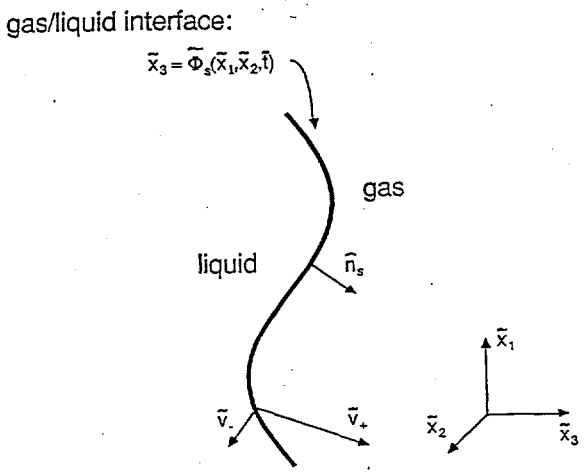

Figure 1. Model geometry.

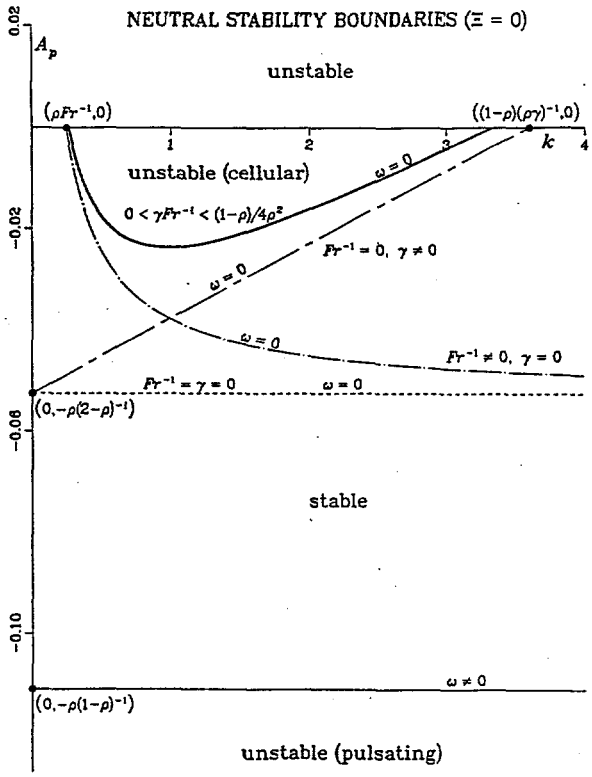

Figure 2. Inviscid hydrodynamic neutral stability boundaries, based on Eq. (11).

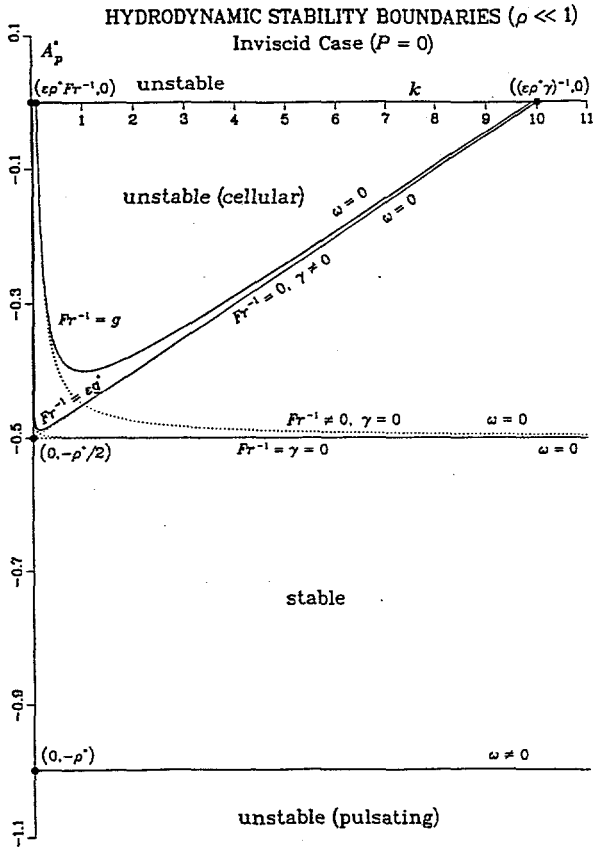

Figure 3. Asymptotic representation of the cellular hydrodynamic stability boundary for the inviscid case, based on Eq. (13).

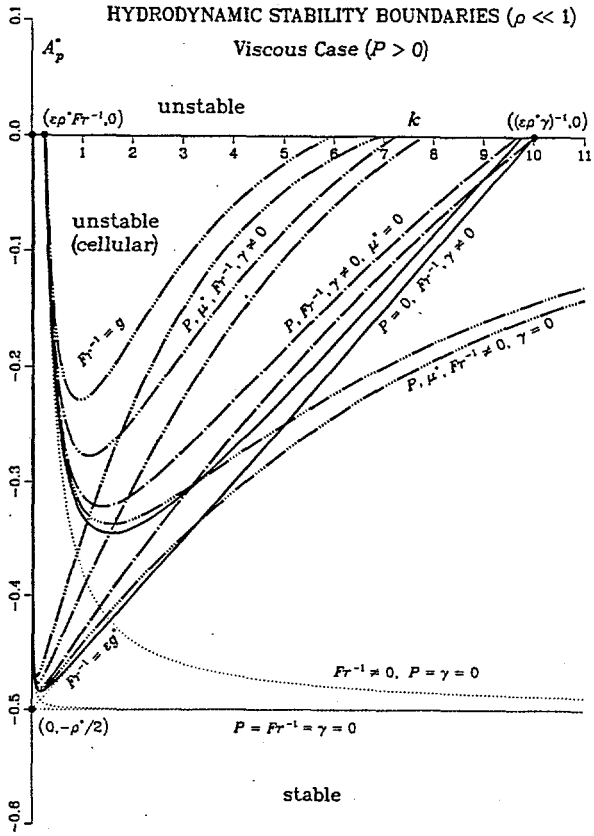

Figure 4. Asymptotic representation of the cellular hydrodynamic stability boundary for the viscous case, based on Eq. (15).